

Microwave-modulated photoluminescence of a two-dimensional electron gas

B. M. Ashkinadze, E. Linder, and E. Cohen

Solid State Institute, Technion-Israel Institute of Technology, Haifa 32000, Israel

L. N. Pfeiffer

Bell Laboratories, Lucent Technologies, Murray Hill, New Jersey 07974, USA

(Received 18 June 2006; revised manuscript received 31 August 2006; published 11 December 2006)

The low-temperature photoluminescence (PL) of GaAs/AlGaAs quantum wells and heterojunctions containing a high mobility two-dimensional electron gas (2DEG) is studied under microwave (mw) irradiation of 36 GHz. The analysis of the mw-modulated PL (MPL) spectra allows us to elucidate the effects of mw radiation on the 2DEG. For low magnetic field strengths ($B < 0.5$ T), we show that the MPL spectral shape is due to energy redistribution of the photoexcited holes, as affected by the mw-heated 2DEG. For the mechanism that causes the nonequilibrium hole-energy redistribution, we propose that it is the interaction of the holes with low-energy acoustic phonons emitted by the mw-heated 2DEG. This underlying physical mechanism gives rise to the optically detected 2DEG cyclotron resonance at low B . For $B > 0.5$ T, optically detected resonances are observed at B values that depend on the 2DEG density, and they occur near integer electron filling factors. We argue that these resonances result from a slight 2DEG density increase under mw irradiation with a concurrent, low-energy PL spectral shift due to small band-gap narrowing.

DOI: [10.1103/PhysRevB.74.245310](https://doi.org/10.1103/PhysRevB.74.245310)

PACS number(s): 73.20.Mf, 71.36.+c, 78.70.Gg

I. INTRODUCTION

The radiative recombination of a two-dimensional electron gas (2DEG) with photoexcited free holes in modulation-doped GaAs/AlGaAs quantum wells (MDQW's) gives rise to photoluminescence (PL) whose spectrum is an effective tool for the study of 2DEG properties. With increasing magnetic field, applied perpendicularly to the 2DEG layer (B_{\perp}), the low-temperature PL spectrum reflects the electron distribution among Landau levels (LLs) and peculiarities due to the integer and fractional quantum Hall effect.¹ For electron filling factor $\nu = 2\pi L_B^2 n_{2D} < 1$ (n_{2D} is the 2DEG density, L_B the magnetic length) additional, high-energy bands appear in the PL spectrum of MDQW's,² and these were recently intensively studied.³⁻⁵

The effectiveness of PL spectroscopy is further enhanced by modulating it by microwave (mw) irradiation. The basic process of mw-induced PL changes in semiconductors is electron heating due to mw absorption by free electrons,⁶ so that the electron temperature T_e exceeds the lattice temperature T_L .⁷ A variety of secondary processes are induced by the heated electrons, among them emission of low-energy acoustic phonons,⁸⁻¹⁰ 2DEG density variation,¹¹ and lattice temperature increase (bolometric effect).

Under B_{\perp} , strong absorption occurs when the mw frequency matches the cyclotron or spin resonances. Then, the T_e dependence on B_{\perp} follows the resonances, and a resonant enhancement of the mw-modulated PL (MPL) intensity occurs. The MPL intensity dependence on B_{\perp} is often used to observe various optically detected resonances (ODR's): cyclotron, dimensional magnetoplasma,¹⁰⁻¹³ and composite fermion and electron spin resonances.¹⁴ These resonances allow the determination of the effective masses, density, and spin of the involved 2DEG states (quasiparticles). Under intense mw irradiation, a remarkable modification of the ODR line shape and the mw-induced PL bistability were observed.^{10,11}

It is therefore clear that an identification of the processes that the 2DEG-photoexcited hole system undergoes under mw irradiation is required to understand the variety of phenomena observed in mw-modulated PL spectroscopy. In particular, the physical processes giving rise to ODR's, which were observed in the spectrally integrated MPL intensity dependence on B_{\perp} ^{14,15} should be studied. It is important to notice that the recently discovered mw-induced resistance oscillations (MIRO's) have stimulated great interest in the underlying physics of the 2DEG interaction with microwaves (Ref. 16 and references therein).

In the following, we present an investigation of the mw-induced PL changes that are observed with increasing magnetic field and mw power in GaAs/AlGaAs MDQW's and heterojunctions (HJ's) containing a 2DEG of various density and very high mobility. In this way we elucidate the physical mechanisms giving rise to various optically (or resistivity¹⁶⁻¹⁸) detected resonances. Since the PL spectrum for MDQW is well described by a convolution of the 2DEG energy distribution function with that of free holes, important information on the mw-induced changes in the 2DEG properties was obtained from the analysis of MPL spectra.

A general impression of the mw-irradiation effects on the PL spectrum can be obtained from Fig. 1. Here, the evolution of the PL [Figs. 1(a) and 1(c)] and MPL [Figs. 1(b) and 1(d)] spectrum with increasing B_{\perp} is demonstrated. In the low-field range ($B_{\perp} < 0.5$ T) the modulation depth is largest at the 2DEG cyclotron resonance, and the entire PL spectrum is mw modulated, mostly in the low-energy part of the spectrum [Fig. 1(b)]. In Sec. III, we discuss the MPL at low B_{\perp} and show that it originates in a hole redistribution in the top valence subband, due to mw heating of the 2DEG. In addition, optically detected resonances are discussed in Sec. IV.

For higher magnetic field ($B_{\perp} > 0.5$ T), mw-induced PL changes are observed only under intense mw irradiation ($P_{mw} > 0.5$ mW) and the MPL spectrum reveals a low-energy

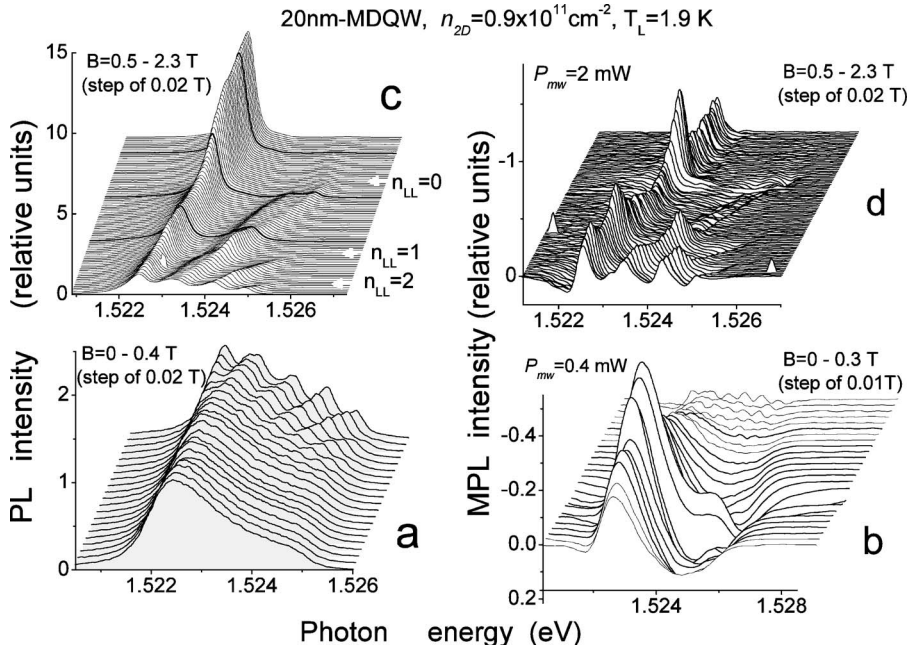


FIG. 1. PL (a), (c) and MPL (b), (d) spectral evolution for 20-nm-wide MDQW ($n_{2D}=0.9 \times 10^{11} \text{ cm}^{-2}$) under B_{\perp} . (b) Low- B_{\perp} range and $P_{mw}=0.4 \text{ mW}$. (d) High B_{\perp} , $P_{mw}=2 \text{ mW}$. The sign of the MPL signals [(b) and (d)] is reversed in order to directly compare the MPL and PL peak intensity dependences on B_{\perp} . The PL and MPL scales are given in relative units.

shift of the PL spectrum [Fig. 1(d)]. We attribute this shift to a very small band-gap energy narrowing (ΔE_g) and further propose that ΔE_g results from a mw-induced 2DEG density increase¹⁵ (band-gap renormalization term).¹⁹ A possible source of additional electrons is the impact ionization of impurities that reside in the AlGaAs-barrier layer (or interface) by mw-heated electrons in the barrier (or in the parallel conducting-doped layer).²⁰ One can also see that the PL and MPL peak intensities in Figs. 1(c) and 1(d) vary in a different way within some B_{\perp} ranges, and new resonances appear in the dependence of the MPL signal on B_{\perp} .¹⁵

The nature of the MPL spectrum at $B_{\perp} > 0.5 \text{ T}$ is considered in Sec. V. Then, the MPL intensity dependence on B_{\perp} giving rise to the ODR's (for $B_{\perp} > 0.5 \text{ T}$) is discussed (Sec. VI). Conclusions are given in Sec. VII.

II. EXPERIMENTAL DETAILS

Several single, modulation-doped GaAs/AlGaAs QW's with well widths of 20–40 nm and HJ's were studied. These samples were grown by molecular beam epitaxy on (001) GaAs wafer. The δ -Si-doped layer is separated from the GaAs/AlGaAs interface by a AlGaAs spacer whose width varies in the range 50–100 nm for different samples. The 2DEG density (n_{2D}) range was 0.2×10^{11} – $2 \times 10^{11} \text{ cm}^{-2}$ and its mobility was $\mu_e=(2-5) \times 10^6 \text{ cm}^2/(\text{V sec})$ at 2 K.

The sample, of a typical size of 1–3 mm, was inserted inside a short-circuited 8-mm waveguide, at the maximum of the mw electric field, which was directed in the 2DEG plane. (A schematic description of the pertinent directions is shown in the inset of Fig. 2). The waveguide was mounted inside a superconducting solenoid. The external magnetic field ($B < 7 \text{ T}$) was applied either perpendicularly to the 2DEG layer (B_{\perp}) or in parallel to it (B_{\parallel}). The sample was immersed in liquid He, and the experiments were done at $T_L=1.9 \text{ K}$. A Gunn diode provided mw radiation at a frequency of 36 GHz

($\omega_i \approx 2.3 \times 10^{11} \text{ sec}^{-1}$). The output power was attenuated so that the incident power P_{mw} was varied from 10 μW to 20 mW. A Ti-sapphire laser with photon energy $E_L = 1.56 \text{ eV}$ (below the AlGaAs-barrier band gap) illuminated the sample through a small hole in the waveguide. The exciting light intensity was low ($< 0.1 \text{ W/cm}^2$). The circularly

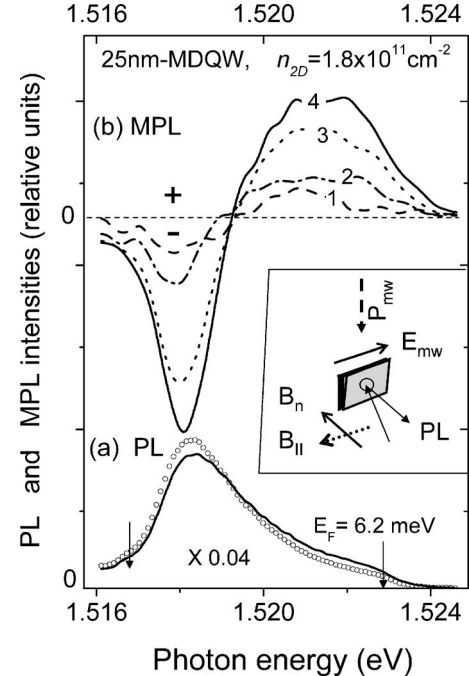


FIG. 2. (a) PL spectra under $B_C=86 \text{ mT}$ for $P_{mw}=0$ (open circles) and $P_{mw}=0.02 \text{ mW}$ (solid line). (b) mw-modulated PL (MPL) spectra under $P_{mw}=0.02 \text{ mW}$ for $B_{\perp}=30 \text{ mT}$ (1), 120 mT (2), and 70 mT (3) and 86 mT (at electron CR) (4). Inset: schematically depicted geometry of the experiment. The PL and MPL intensities are in relative units with the ratio number written at the bottom.

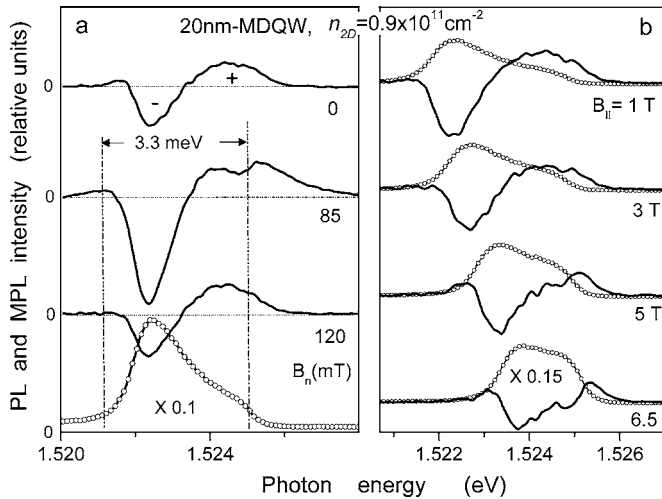


FIG. 3. (a) PL (open circles) and MPL spectra of a 20-nm-wide MDQW for three B_{\perp} values at $P_{mw} = 0.05 \text{ mW}$ and $T_L = 1.9 \text{ K}$. (b) In-plane magnetic field: PL and corresponding MPL spectra at $P_{mw} = 0.1 \text{ mW}$ for several $B_{||}$ values. The spectra are vertically shifted for clarity.

polarized (σ^- or σ^+) PL was analyzed by a double-grating spectrometer with a spectral resolution of 0.03 meV. The PL spectra were detected with a cooled charge-coupled-device (CCD) camera, and the mw-modulated PL spectrum was obtained as the difference of two successive PL spectra, in the presence and in the absence of mw irradiation.¹⁴

III. MICROWAVE MODULATED PL BY 2DEG HEATING: THE ROLE OF NON-EQUILIBRIUM PHONONS

A. Experimental results

Figure 2 displays several PL and MPL spectra of a single-side modulation-doped QW (25 nm wide) having $n_{2D} \approx 1.8 \times 10^{11} \text{ cm}^{-2}$. In Fig. 2(a), the 2DEG-free hole PL spectra obtained with and without mw irradiation are shown. The spectral width of the PL band is 6.2 meV, and this value is close to the 2DEG Fermi energy E_F . The MPL spectra were measured under incident mw power of $\approx 20 \mu\text{W}$ at several B_{\perp} values: $B_{\perp} < B_C$, $B_{\perp} = B_C$ and $B_{\perp} > B_C$ where $B_C = m_e^* c \omega_i / e = 86 \text{ mT}$ is the B_{\perp} value for the electron cyclotron resonance (CR) in GaAs. (m_e^* is the electron effective mass, c the light velocity). The mw-modulated PL amplitude is highest at B_C , while it is $\approx 1\%$ of the PL peak intensity out of the CR (at $B_{\perp} = 30 \text{ mT}$). These are the lowest mw-induced PL changes that were detectable by subtracting two successive PL spectra [such as those shown in Fig. 2(a)].

In Fig. 3, the MPL and PL spectra of a two-sided modulation-doped 20-nm-wide QW sample that has a 2DEG density $n_{2D} \approx 1 \times 10^{11} \text{ cm}^{-2}$ are shown for B_{\perp} (a) and for in-plane $B_{||}$ (b). The 2DEG-free hole PL spectral width is 3.3 meV, a value $\sim E_F$. For B_{\perp} , the MPL spectra were measured under $P_{mw} = 50 \mu\text{W}$ at three B_{\perp} values, and for $B_{||}$, P_{mw} was $\approx 100 \mu\text{W}$.

The MPL spectra in Figs. 2 and 3(a) show a PL intensity decrease in the low-energy part of the spectrum (negative MPL signal) and its increase at higher photon energies. The MPL spectrum spreads to higher photon energies either with increasing mw power or at B_C when the mw absorption by the 2DEG is the highest. These features of the MPL spectra, in particular the largest modulation depth of the PL at the electron cyclotron resonance condition, indicate that the basic effect of mw irradiation is due to the 2DEG mw absorption. It leads to an increase of the 2DEG temperature T_e .

It should be noted that the spectrally integrated MPL signal is nearly zero. This means that the 2DEG recombines mainly radiatively and the mw-induced PL changes are not due to activation of nonradiative recombination channels (as is often observed in undoped QW's or bulk semiconductors⁶).

If mw irradiation would affect a T_e increase alone, then the expected MPL signal would be observed only in the spectral range around E_F since all the electron states with energy $E < E_F$ are occupied. However, this is not observed for the high-density sample, as seen in Fig. 2(b). For the low-density sample, only a minor PL change (such as the small dip in the positive background just below E_F and the tail extending above E_F) is seen under higher P_{mw} or for fields around B_C [middle MPL spectrum in Fig. 3].

The strongest mw-induced PL modulation signals occur at energies much below E_F , and actually the MPL spectrum spreads over the entire PL energy range (Figs. 2 and 3). At low PL energies, the electrons occupying states with $E \ll E_F$ participate in the optical transitions. These are not affected by mw heating, and we thus conclude that the energy redistribution of the photoexcited holes along the dispersion curve of the hh1 valence subband gives rise to the observed MPL spectrum. The strongest modulation occurs at B_C when the mw heats mainly the 2DEG. Therefore, hole redistribution is caused by energy transfer from the hot 2DEG, and it is an indirect (secondary) effect of mw irradiation on the PL.

More information on the hole-energy redistribution induced by mw irradiation is obtained by studying the MPL under a magnetic field applied in parallel to the 2DEG. Recently, we showed that the 2DEG PL spectrum is modified with increasing $B_{||}$ and the PL intensity near E_F increases.²¹ Figure 3(b) shows the evolution of the PL (circles) and MPL (solid curves) spectra with increasing $B_{||}$. A pronounced effect of $B_{||}$ on the MPL spectrum is observed, although the 2DEG temperature is not affected by $B_{||}$ (which is parallel to the mw electric field). In particular, a MPL dip appears near E_F at $B_{||} = 6.5 \text{ T}$ and the MPL amplitude decreases with $B_{||}$. The reason for such PL changes is that the electrons of $E \approx E_F$ can recombine with valence holes of various energies due to the relative shift of the conduction- and valence-band dispersion curves under $B_{||}$.²¹ Then, the energy and amount of valence holes available for recombination with the electron vary with $B_{||}$, so that the PL at any photon energy depends on the energy-averaged hole redistribution. Below, we will compare these experimental findings with calculated MPL spectra.

The MPL spectra obtained under both B_{\perp} and $B_{||}$ are explained by the energy redistribution of valence holes: the low-energy hole population decreases while the high-energy

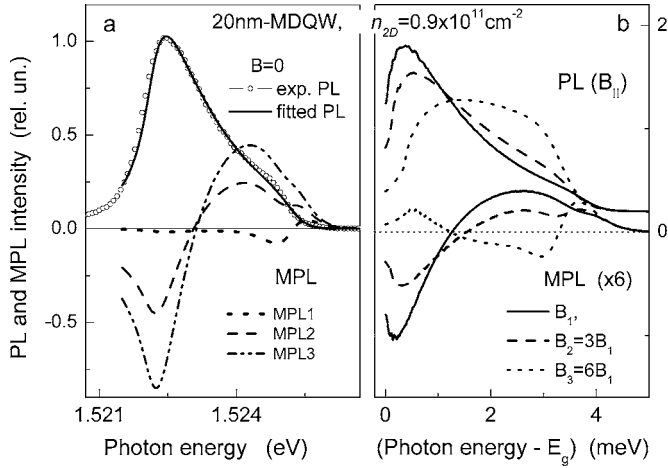


FIG. 4. (a) The measured PL spectrum ($P_{mw}=0$) at $T_L=1.9$ K (open circles) and the calculated one (solid line) for $T_e=T_L$, $T_h^0=2.55$ K. The MPL1, MPL2, and MPL3 spectra are calculated for $T_e-T_L=0.3$ K and $T_h=2.55$ ($=T_h^0$), 2.8, and 3 K, respectively. (b) Calculated PL and MPL spectra for three in-plane B_{\parallel} values. $T_e-T_L=0.5$ K and $T_h=3$ K [these temperatures are higher than that in (a) since the MPL spectra for B_{\parallel} were obtained at higher P_{mw} ; see Fig. 3].

one increases. We shall examine this proposition by calculating first the MPL spectrum and then considering the mechanism responsible for energy transfer from the heated 2DEG to the holes.

B. Numerical simulation of the PL and MPL spectra: Nonthermal photoexcited hole distribution

We use a simplified model for calculating the PL spectrum that arises from the radiative recombination of the 2DEG with holes in a single, parabolic valence subband (hh1). In the case of direct optical transitions, the PL spectrum is well described by the product of the electron and hole distribution functions. Taking into account an energy-independent joint density of states $D(\hbar\omega)=1/2 + 1/\pi \arctan[(\hbar\omega-E_g)/\Gamma]$ with a broadening parameter Γ , the PL intensity at photon energy $\hbar\omega=E_g+\varepsilon_e+\varepsilon_h$ is²²

$$I(\hbar\omega) \propto D(\hbar\omega)f(\varepsilon_e)f(\varepsilon_h). \quad (1)$$

Here E_g , ε_e , and ε_h are the band gap and electron and hole in-plane energy, respectively. $f(\varepsilon_e)$ and $f(\varepsilon_h)$ are the Fermi distribution function for 2D electrons and the Boltzmann distribution function for nondegenerate (low-density) photoexcited holes. The distribution functions are characterized by effective temperatures for the electrons (T_e) and the holes (T_h). The direct optical transitions with a given $\hbar\omega$ occur at $\hbar k_e = \hbar k_h = 2\mu(\hbar\omega - E_g)^{1/2}$. Here $1/\mu = 1/m_e + 1/m_h$ is the reduced electron-hole effective mass with the effective electron mass value of $m_e = 0.0665m_0$ and the effective heavy-hole mass in the hh1 subband $m_h = 0.35m_0$. The energies in Eq. (1) are $\varepsilon_e = \mu/m_e(\hbar\omega - E_g)$, and $\varepsilon_h = \mu/m_h(\hbar\omega - E_g)$. The PL

spectrum of the MDQW's is well fitted by Eq. (1) for 2DEG densities above $n_{2D} = 5 \times 10^{10} \text{ cm}^{-2}$, since then the electron-hole interaction is screened by the 2DEG and its contribution can be left out.

Figure 4(a) shows the experimentally measured PL spectrum at $T_L=1.9$ K ($P_{mw}=0$, circles), which is fitted with the calculated spectrum (solid line) using Eq. (1) with $\Gamma = 0.25$ meV. In the absence of mw irradiation, such a fitting procedure gives the proper n_{2D} value and the extracted $T_e^0 = 1.9$ K while $T_h^0 = 2.55$ K, which exceeds T_e^0 and T_L . This is interpreted as a result of a nonequilibrium distribution of photoexcited holes. It is further supported by the observation of PL bands due to the transitions between electrons in occupied Landau levels [marked with $n_{LL}=1, 2, 3, \dots$ in Fig. 1(c)] and high-energy, nonthermalized holes that occupy the corresponding valence-band Landau levels.²³

At low temperature, the energy relaxation of photoexcited holes occurs by emission of low-energy acoustic phonons. The lifetime associated with this process exceeds the 2DEG-hole radiative lifetime (due to the small e-h separation in MDQW's).¹ Thus, the photoexcited holes recombine with the 2DEG before the Boltzmann distribution function corresponding to the ambient T_L is established, and T_h in Eq. (1) has the sense of an "effective temperature." In contrast, T_e is established much faster due to the scattering of photoexcited (or mw-heated) electrons within the 2DEG, and the 2DEG distribution can be well characterized by T_e . For low photoexcitation intensities and in the absence of mw irradiation, $T_e^0 \approx T_L$.

As the 2DEG gains energy from the mw electric field, T_e can easily exceed T_L .⁷ This results from the low rate of 2DEG energy losses by acoustic phonon emission at low lattice temperature. We assume that the mw effect on the PL comes from the increased T_e and accompanying increase of the effective T_h .

In order to simulate the MPL spectrum, several PL spectra were calculated in which T_e and T_h vary, and then, these were subtracted from the spectrum that gives the best fit to the observed PL in the absence of mw irradiation. The spectra were calculated imposing the condition that they maintain the same integrated intensity (namely, a 100% quantum efficiency). The result is a series of calculated MPL spectra as shown in Fig. 4(a). It can be clearly seen by comparing the calculated MPL spectra with the experimental spectra in Fig. 3(a), that increasing T_e alone (namely, the sole effect of mw irradiation is heating of the 2DEG) does not reproduce the correct MPL spectral shape. In particular, the MPL1 spectrum in Fig. 4(a) was calculated for $T_e-T_L=0.3$ K while maintaining a fixed T_h^0 . On the other hand, the MPL spectra calculated with $T_e-T_L=0.3$ K and $T_h=2.8$ K and 3 K [dashed and dash-dotted lines in Fig. 4(a)] reproduce quite well the main features of the observed MPL spectra as one can conclude from comparing Figs. 2(a) and 3(a) with Fig. 4(a).

In the case of parallel B_{\parallel} , a similar simulation procedure for the MPL spectra was performed by using Eq. (4) of Ref. 21. Figure 4(b) displays the simulated PL (in the absence of mw) and the MPL spectra for three B_{\parallel} values assuming $T_e = 2.4$ K and $T_h = 3$ K, which do not vary with B_{\parallel} . One can conclude that the calculated MPL spectral evolution reflects

the main peculiarities seen in the MPL spectra obtained at $P_{mw}=0.1$ mW [Fig. 3(b)]. In particular, the appearance of a dip near E_F and the MPL amplitude decrease with increasing B_{\parallel} are well simulated. Still, a perfect fit cannot be obtained by just varying the effective T_h , and this indicates that the assumed Boltzmann distribution for the holes is not an accurate approximation. It should be underlined that the observed MPL spectra cannot be fitted by varying only T_e .

Presenting the experimental spectra together with the simulated MPL spectra allows us to conclude that it is the hole-energy redistribution that is mostly responsible for the observed PL changes—namely, for the spectral MPL line shape under mw heating of the 2DEG. The question is how is the hole energy redistribution affected by mw irradiation?

Direct mw heating of valence holes (under the low P_{mw} used) is negligible due to the large hole effective mass and, thus, to the much lower hole mobility. Direct inelastic scattering of holes with hot electrons (having wave vectors near k_F) is inefficient for a degenerate 2DEG,²⁴ in particular for the asymmetric MDQW structures where the 2DEG and holes are spaced apart.

Thus, in a steady state, all mw power gained by the 2DEG is dissipated by emission of acoustic phonons. The characteristic energy of the acoustic phonons emitted by the 2DEG at $T_e < 10$ K is $\varepsilon \approx S(2E_{Fm_e})^{0.5} \approx 0.2-0.3$ meV (S is the sound velocity).²⁵ At low temperature, these nonequilibrium low-energy phonons propagate ballistically throughout the sample, maintaining a nonequilibrium energy distribution since their lifetime τ_b is determined only by the phonon scattering on the sample boundaries: $\tau_b \approx L/S \sim 10^{-7}$ sec (for the characteristic sample size $L=0.5$ mm). Thus, the population of the low-energy acoustic phonons significantly exceeds the equilibrium one.^{25,26}

The nonequilibrium phonons are subsequently absorbed by the valence holes, and this causes the nonequilibrium hole redistribution. A similar effect of nonequilibrium phonons on the distribution function of carries was theoretically considered in Ref. 27. Thus, we propose that an indirect 2DEG-hole interaction mediated by the nonequilibrium phonons results in a hole-energy redistribution, and therefore, the population of low-energy hole states decreases while that of higher-energy ones increases, as the MPL spectrum reveals.

The proposed mechanism is specific to the 2DEG since the nonequilibrium phonon flux is proportional to the 2DEG density. In contrast, at low electron density or for undoped semiconductors, direct hot electron-exciton (hole) scattering is responsible for the observed mw-induced PL changes.⁶

Therefore, it is proposed that nonequilibrium phonons play an important role in all cases where 2DEG heating occurs (such as intense interband or intersubband light absorption, under dc current flow or mw irradiation). In particular, they should be taken into account in the physical mechanisms giving rise to the recently studied mw-induced resistance oscillations.¹⁶ The latter are usually observed at mw powers considerably higher than the P_{mw} values of 10–20 μ W used here and that induce the PL changes due to the generation of nonequilibrium phonons by the mw-heated 2DEG.

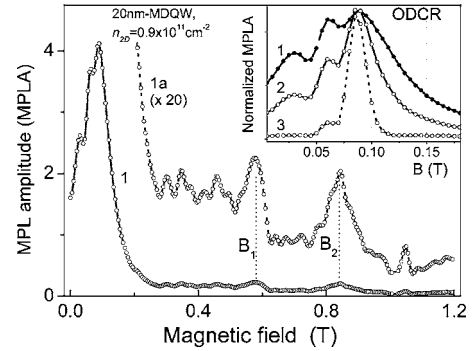


FIG. 5. Integrated MPL amplitude (MPLA) dependence on B_{\perp} . The inset shows the MPLA traces near the ODCR field. The MPLA traces 1, 2, and 3 are obtained by integrating the MPL amplitude over the entire spectrum and over the low-energy (negative) and the high-energy (positive) parts of the MPL spectrum, respectively [as can be seen in Fig. 3(a)].

IV. OPTICALLY DETECTED RESONANCES

It is well known that mw absorption by electrons exhibits an electron CR at B_C .²⁸ The CR transforms into a dimensional magnetoplasma resonance (DMPR) with increasing electron density.^{28,29} For the 2DEG, the DMPR field is $B_R = B_C[1 - Len_{2D}c/\omega_e \epsilon a B_C]$ where L , ϵ , and a are the numerical depolarization factor, the dielectric constant, and the characteristic length of the sample, respectively. The DMPR is very useful for contactless 2DEG study.^{11,13} Under intense mw irradiation, it is accompanied by a resonant $T_e(B_{\perp})$ dependence. The strongest mw-induced PL changes are observed at the electron DMPR, and various other resonances of the 2DEG were investigated by an optical detection technique.¹⁰⁻¹⁵

In this method, the absolute value of the MPL intensity is integrated within some spectral window (or over the entire MPL spectrum) and the resulting integrated MPL amplitude (MPLA) is plotted as a function of B_{\perp} . The inset of Fig. 5 shows MPLA (B_{\perp}) traces obtained for three different spectral windows. Each displays a strong optically detected electron DMPR and additional lower-field resonances due to other DMPR modes or DMPR subharmonics.¹³ These additional resonances are observable by ODR spectroscopy due to the strong nonlinear dependence of the MPL intensity (and its spectrum) on mw-absorbed power. Moreover, as B_{\perp} sweeps through the resonance, the MPL spectrum is modified (see Figs. 2 and 3), and the ODR line shape (even its position) depends on the spectral window in which the MPLA (B_{\perp}) trace was obtained as can be seen in the inset of Fig. 5.

For $B_{\perp} > B_R$, the MPL intensity decreases, as can be deduced by comparing the scales of Figs. 1(b) and 1(d) (see also curves 1 and 1a in Fig. 5). This is due to the reduced mw absorption by the 2DEG and, consequently, to less 2DEG heating. In the classical Drude approach, the electron mw absorption decreases as $1/(\mu_e B_{\perp})^2$ (where μ_e is the 2DEG mobility). In the quantum mechanical approach, which applies at high B_{\perp} , this decrease is due to a reduced overlap between the broadened Landau levels. For example, at $B_{\perp}=0.5$ T, the inter-Landau level LL energy spacing is

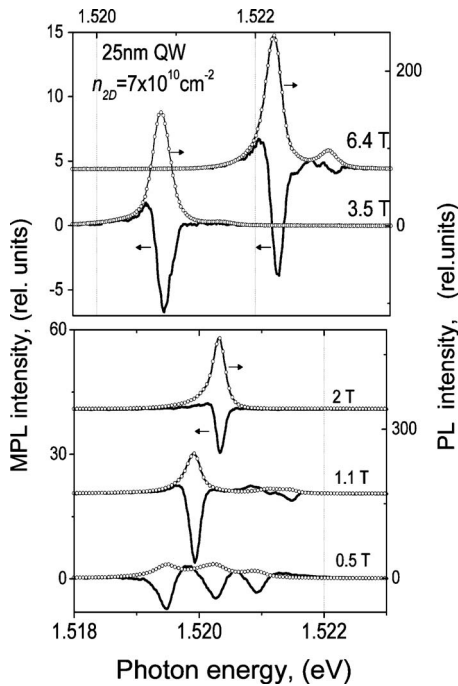


FIG. 6. The MPL and PL spectra for several B_{\perp} values and at $P_{mw}=1$ mW. Vertical scales show the relative values of the MPL and PL intensities (left and right scale, respectively).

~ 6 times larger than the mw-photon energy at 36 GHz. As shown by curve 1 in Fig. 5, the MPL intensity is greatly reduced (~ 100 fold) for $B_{\perp} > 0.3$ T. Thus, the mw-modulated PL signal was less than 1% of the PL intensity (at $P_{mw} \approx 0.2$ mW).

In order to observe mw-induced effects at higher B_{\perp} (above 0.5 T), mw-irradiation power $P_{mw} > 0.5$ mW was used. Then, the absolute value of the MPL signal integrated over the entire MPL spectrum (MPLA vs B_{\perp} dependence) reveals several weak resonance bands that appear at certain B_{\perp} values on the fluctuating background (at B_1 and B_2 values in Fig. 5).¹⁵ In Fig. 1(d), the resonant enhancements of the MPL peak intensity are also seen.

These resonant mw-induced PL changes detected by the MPLA trace cannot be attributed to 2DEG heating since mw absorption by the magnetized 2DEG is very low. A weak 2DEG heating might come from mw-induced hopping conductivity between localized states, which was observed in low-mobility samples.³⁰

In general, 2DEG spin resonance bands can be observed at certain B_{\perp} values, on the weak mw-induced background, by using the ODR technique.^{14,31} Similar behavior of mw-modulated signals versus B_{\perp} is observed in the case of resistance-detected 2DEG spin resonance^{17,18} or in the optically detected mw-induced spin resonance in bulk semiconductors.³² Such a background results from the mw heating of the low-mobility electrons,³² but this is not the case for the high-mobility 2DEG. Thus, the nature of the mw-induced PL changes at high B_{\perp} should be examined in order to identify the MPLA resonance bands and to understand the origin of the strong fluctuating MPLA background (curve 1a in Fig. 5).

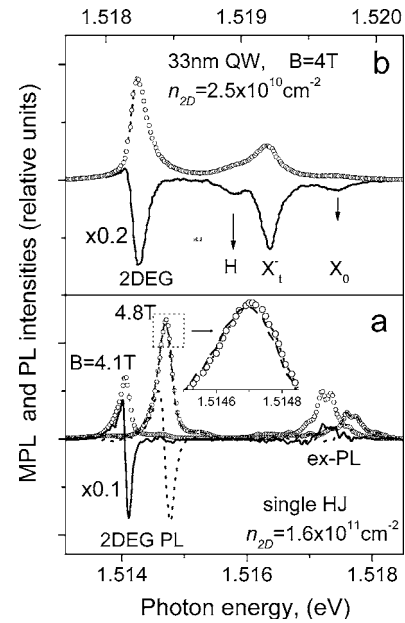


FIG. 7. (a) PL (open circles) and MPL spectra for heterojunction at $B_{\perp}=4.1$ and 4.8 T (solid and dotted lines, respectively). (b) The PL and MPL spectra of a low-density 33-nm-wide MDQW at $B_{\perp}=4$ T. $P_{mw}=1$ mW.

V. mw-INDUCED PL CHANGES AT HIGH B

The origin of the mw-induced PL modulation observed for $B_{\perp} > 0.5$ T is identified by analyzing the MPL spectra. In Fig. 6, the PL and MPL spectra of 25-nm-wide MDQW ($n_{2D}=0.7 \times 10^{11}$ cm⁻²) for several B_{\perp} values and under $P_{mw} \sim 1$ mW are presented. At $B_{\perp}=0.5$ T, the mw-modulated amplitude is $\sim 20\%$ of the PL intensity, and it mainly reflects the mw-induced broadening of the PL lines corresponding to recombination from $N_{LL}=0, 1, 2$ Landau levels. We attribute this broadening to a slight 2DEG heating still occurring at high mw power (≈ 1 mW). With increasing B_{\perp} , the PL line broadening diminishes and the mw-modulation depth decreases since mw absorption reduces with B_{\perp} .

At $B_{\perp} > 2$ T, the PL spectrum is due to the 2DEG-hole transitions between the lowest e-h Landau levels and the mw-modulation depth is less than $\sim 5\%$. Then, the MPL spectra at 2, 3.5, and 6.4 T show a small positive signal in the low-energy part and a large negative signal in the high-energy part of the spectrum. This means that the PL line shifts to lower photon energy by 0.02–0.08 meV. At $B_{\perp}=6.4$ T ($\nu \sim 0.5$), an additional high-energy PL band (H band⁵) is seen in the PL spectrum and the entire PL spectrum is shifted under mw irradiation (Fig. 6). The MPL spectra of the 20-nm-wide MDQW show similar behavior [Fig. 1(d)].

The mw-induced PL energy shift is very small, and it can be clearly detected only for narrow PL lines in high-quality samples. Moreover, only the PL lines due to the 2DEG-hole recombination exhibit such a redshift, it is not observed in the excitonlike transitions. Figure 7(b) displays the PL and MPL spectra for the low-density 33-nm-wide MDQW ($n_{2D}=2.5 \times 10^{10}$ cm⁻²) where excitonlike (charged and neutral

excitons X^- and X^0) and 2DEG PL bands coexist at $B_\perp > 3.5$ T ($\nu < 0.5$).³⁻⁵ The MPL spectrum shows that the 2DEG (and H) PL bands are affected differently by mw irradiation as compared to the X^- and X^0 bands. The former show a shift while the charged (and neutral) exciton PL lines exhibit only a decreased PL intensity ($\sim 10\%$) under mw irradiation. It is worth noting that similar PL spectral shifts were previously observed when n_{2D} was varied by optical depletion, and the different response of the excitonic and 2DEG PL to the n_{2D} variation was explained by the appearance of 2DEG puddles in photoexcited MDQWs.⁵

This difference in the MPL spectra for both transitions is clearly observed in the single heterojunction. Its spectrum consists of a low-energy PL band due to the 2DEG which occupies the lowest Landau level and of high-energy PL lines due to bulk excitons in the GaAs buffer layer.³³ The MPL spectra in Fig. 7(a) (solid and dotted lines) show a low-energy shift for the 2DEG PL band, while the exciton PL lines do not shift. The inset of Fig. 7(a) displays an enlarged part of the PL spectra in the presence (dashed line) and in the absence (circles) of mw irradiation, and it demonstrates how small the mw-induced PL shift is. The exciton PL is practically unaffected by mw at high B_\perp (> 1 T), and this is evidence of negligible 2DEG mw heating.¹⁰ On the other hand, a redshift of the 2DEG PL band was observed for samples with a higher 2DEG density,³³ and thus we conclude that the mw-induced PL shift comes from a slight 2DEG density increase. It is worth noticing, that the MPL peak intensity does not vary proportionally to the PL as B_\perp increases [one can see this by comparing the PL and MPL spectra for two B_\perp values in Fig. 7(a)]. This means that the mw-induced spectral PL shift is sensitive to the B_\perp value and it slightly decreases with B_\perp .

We attribute the spectral redshift to a 2DEG density increase that is induced by intense mw irradiation ($P_{mw} > 0.5$ mW).¹⁵ The increased n_{2D} leads to a small band-gap energy reduction that results from an increased electron-electron-interaction (band-gap renormalization effect¹⁹). As is seen from Figs. 6 and 7 the mw-induced redshift of the PL spectrum is less than 0.1 meV. From this value of ΔE_g , the estimated increase in n_{2D} (Ref. 19) is less than 3×10^9 cm⁻² (at $P_{mw} = 1$ mW). It should be noted that at low B_\perp , when 2DEG mw heating is most effective, the 2DEG density can be reduced under mw irradiation.¹¹

The mw-induced n_{2D} increase is likely caused by injection of additional electrons from the AlGaAs barrier layer or from the GaAs/AlGaAs interface. These electrons appear in the QW as a result of impact ionization of impurities that reside in the barrier layer (or interface) by residual (in the parallel δ -doped layer) or photoexcited electrons that are mw heated.²⁰ Since the mobility of electrons in the barrier layer is low, such a heating occurs only under increased P_{mw} and it decreases slightly with B_\perp .

In our previous study of mw absorption in undoped photoexcited GaAs heterostructures we observed a mw-induced avalanche impurity breakdown as the mw power exceeds the threshold value of 0.5–1 mW.²⁰ In the present experiments, the MPL peak intensity increases superlinearly with P_{mw} (see also Ref. 14). This signifies a nonlinear dependence of the

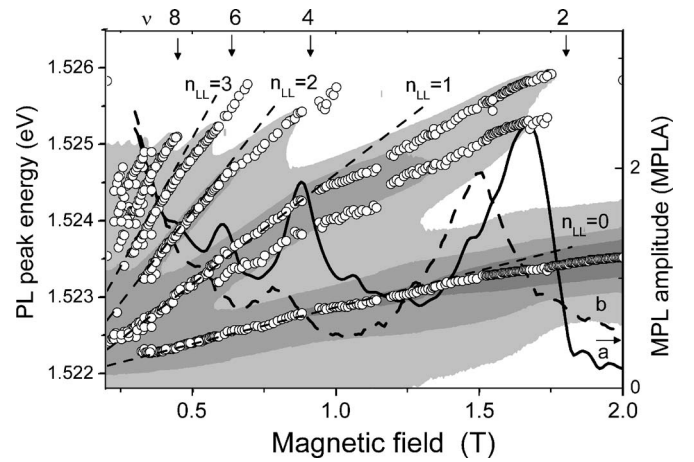


FIG. 8. Contour PL plot (gray scale), PL peak energy (open circles), and MPLA dependence (*a* and *b* curves) on B_\perp for a 20-nm-wide MDQW (the same as in Fig. 3), $P_{mw} = 1$ mW. The straight dashed lines are the best fit to the Landau-level behavior: $E = E_g + \hbar \omega_c (n_{LL} + 1/2)$ where n_{LL} is the integer LL number and $(\hbar \omega_c / 2) / B_\perp = 0.00096$ eV/T. The filling factors ν are shown on the top.

injected electron density on mw power, and it is typical of avalanche impurity breakdown. The proposed mechanism of electron injection due to impurity impact ionization is expected to cause a strongly fluctuating MPL signal, and this explains the origin of the fluctuating MPLA background seen in curve 1a in Fig. 5.

Therefore, at $P_{mw} > 0.5$ mW, the main mw effect on the magneto-PL is attributed to the mw-induced n_{2D} change. At $P_{mw} < 0.5$ mW, the PL mw-modulation depth was less than 1% (for $B > 1$ T), and this restricted detection of mw-induced PL modulation at lower P_{mw} .

We also note that the MPL line shape shown in Figs. 6 and 7 was the same for both σ^- - and σ^+ -PL components. This eliminates the possibility that the observed MPL is due to a mw-induced electron spin flip that results from the electron interacting with the mw-magnetic-field component.¹⁷ Electron spin flip would have resulted in a σ^- -PL intensity decrease accompanied by a σ^+ -PL intensity increase which is not observed.

VI. NATURE OF THE mw-INDUCED ODR AT HIGH B

It is left now to explain the origin of the resonance bands observed in the MPLA dependence on B_\perp at high fields [Figs. 1(d), 5, and 8]. In order to do so we combine in Fig. 8 the fan diagram of the PL peak energy (open circles) and the MPLA traces (solid and dashed curves), both plotted as a function of B_\perp . In order to appreciate the effect of Landau-level filling, the fan diagram is appended by a contour plot using a three 3-grade gray scale for the PL intensity. The PL energy and the MPLA trace shown by the solid curve were obtained under photoexcitation below the AlGaAs barrier layer (Ti:sapphire laser). One can see that the resonances in the MPLA trace, the ODR fields, are close to the B_\perp values corresponding to even-integer electron filling factors: ν

$\sim 2, 4, 6, 8$. The MPLA trace shown by the dashed curve was obtained under illumination by an He-Ne laser when n_{2D} was reduced by optical depletion.^{1,5} The ODR's are shifted as the ν values move to lower B_{\perp} with decreasing n_{2D} . Several studied MDQW samples having various n_{2D} show the ODR's occurring in the vicinity of even ν .¹⁵

We propose that the MPLA resonance bands appear at B_{\perp} values for which the magneto-PL spectrum responds most sensitively to the 2DEG density variation. In other words, the MPL intensity increases when the mw-modulated n_{2D} causes the largest change in the PL spectrum. It usually occurs in the vicinity of integer ν values, so that a slight change in n_{2D} gives rise to significant PL spectral changes.

In order to verify this, the B_{\perp} derivative of the magneto-PL spectra was numerically obtained: each PL spectrum measured at B_{\perp} was subtracted from that measured at $B_{\perp} + \Delta B_{\perp}$ (where ΔB_{\perp} is equal to 0.01 T). Then, these B_{\perp} -modulated spectra were integrated and the obtained amplitudes were plotted as MPLA vs B_{\perp} . This procedure reproduces the PL spectral shift to lower B_{\perp} with increasing n_{2D} , as was observed in our previous study.⁵ Such a procedure generates the "fake" ODR's that are similar to those obtained under mw irradiation.

Thus, we conclude that the MPLA resonance bands emerge at the B_{\perp} values where the energy of the 2DEG-hole system is most sensitive to a variation of n_{2D} . For instance, any kinks in the fan diagram or the 2D-electron redistribution between LL's near integer ν values can generate these

fake ODR's when mw irradiation affects the 2DEG parameters.

VII. CONCLUSIONS

Microwave irradiation of heterostructures containing a 2DEG gives rise to changes in the low-temperature PL spectrum. At low B , when mw radiation of $P_{mw} > 20 \mu\text{W}$ heats the 2DEG, the MPL spectra reveal a hole-energy redistribution. For the mechanism that causes this redistribution, we propose that it is the interaction of the holes with nonequilibrium, low-energy acoustic phonons emitted by the mw-heated 2DEG. This underlying physical mechanism is responsible for the optically detected 2DEG cyclotron resonance at low B . At higher B_{\perp} , as the 2DEG heating becomes inefficient, the mw-induced effect on the PL spectrum results from a 2DEG density increase due to electron injection from the AlGaAs barrier layer. This n_{2D} increase leads to a low-energy magneto-PL spectral shift and can simulate optically detected resonances in the MPLA dependence on B_{\perp} .

ACKNOWLEDGMENTS

The research at the Technion was done in the Barbara and Norman Seiden Center for Advanced Optoelectronics and was supported by the Israel-U.S. Binational Science Foundation (BSF), Jerusalem. B.M.A. acknowledges support by a grant under the framework of the KAMEA Program.

-
- ¹I. V. Kukushkin and V. B. Timofeev, *Adv. Phys.* **45**, 147 (1996).
²B. B. Goldberg, D. Heiman, M. Dahl, A. Pinczuk, L. Pfeiffer, and K. West, *Phys. Rev. B* **44**, 4006 (1991); D. Heiman, A. Pinczuk, H. Okamura, M. Dahl, B. S. Dennis, L. N. Pfeiffer, and K. W. West, *Physica B* **201**, 315 (1994).
³G. Yusa, H. Shtrikman, and I. Bar-Joseph, *Phys. Rev. Lett.* **87**, 216402 (2001).
⁴C. Schuller, K. B. Broocks, Ch. Heyn, and D. Heitmann, *Phys. Rev. B* **65**, 081301(R) (2002).
⁵B. M. Ashkinadze, E. Linder, E. Cohen, A. B. Dzyubenko, and L. N. Pfeiffer, *Phys. Rev. B* **69**, 115303 (2004); B. M. Ashkinadze, V. V. Rudenkov, P. C. M. Christianen, J. C. Maan, E. Linder, E. Cohen, and L. N. Pfeiffer, *Phys. Status Solidi C* **1**, 514 (2004).
⁶M. Godlewski, W. M. Chen, and B. Monemar, *Crit. Rev. Solid State Mater. Sci.* **19**, 241 (1994); B. M. Ashkinadze, V. V. Bel'kov, and A. G. Krasinskaya, *Fiz. Tekh. Poluprovodn. (S.-Peterburg)* **24**, 883 (1990) [*Sov. Phys. Semicond.* **24**, 555 (1990)]; B. M. Ashkinadze, E. Cohen, A. Ron, and L. N. Pfeiffer, *Phys. Rev. B* **47**, 10613 (1993).
⁷E. Conwell, *High Field Transport in Semiconductors* (Academic Press, New York, 1967); F. Neppel, J. P. Kotthaus, and J. F. Koch, *Phys. Rev. B* **19**, 5240 (1979); D. R. Leadley, R. J. Nicholas, J. J. Harris, and C. T. Foxon, *Semicond. Sci. Technol.* **4**, 879 (1989).
⁸A. J. Kent, in *Hot Electrons in Semiconductors: Physics and Devices*, edited by N. Balkan (Oxford University Press, Oxford, 1997), p. 81.
⁹A. V. Akimov, L. J. Challis, J. Cooper, C. J. Mellor, and E. S. Moskalenko, *Phys. Rev. B* **45**, 11387 (1992).
¹⁰B. M. Ashkinadze, E. Linder, and V. Umansky, *Phys. Rev. B* **62**, 10310 (2000); Proceedings of the 26th ICPS, (Edinburgh, 2002), Institute of Physics Conference Series Number 171.
¹¹B. M. Ashkinadze and V. Yudson, *Phys. Rev. Lett.* **83**, 812 (1999); B. M. Ashkinadze, V. Voznyy, E. Linder, E. Cohen, A. Ron, and L. N. Pfeiffer, *Phys. Rev. B* **64**, 161306(R) (2001); B. M. Ashkinadze, A. Nazimov, E. Cohen, A. Ron, and L. N. Pfeiffer, *Phys. Status Solidi A* **164**, 523 (1997).
¹²M. Godlewski, T. Lundstrom, Q. X. Zhao, W. M. Chen, P. O. Holtz, B. Monemar, and T. G. Anderson, *Phys. Rev. B* **52**, 14688 (1995).
¹³S. I. Gubarev, I. V. Kukushkin, S. V. Tovstonog, M. Yu. Akimov, J. H. Smet, K. von Klitzing, and W. Wegscheider, *JETP Lett.* **72**, 324 (2000); I. V. Kukushkin, J. H. Smet, S. A. Mikhailov, D. V. Kulakovskii, K. von Klitzing, and W. Wegscheider, *Phys. Rev. Lett.* **90**, 156801 (2003); V. A. Kovalskii, S. I. Gubarev, I. V. Kukushkin, S. A. Mikhailov, J. H. Smet, K. von Klitzing, and W. Wegscheider, *Phys. Rev. B* **73**, 195302 (2006).
¹⁴I. V. Kukushkin, J. H. Smet, K. von Klitzing, and W. Wegscheider, *Nature (London)* **415**, 409 (2001); I. V. Kukushkin, J. H. Smet, D. S. Lyne Abergel, V. I. Fal'ko, W. Wegscheider, and K. von Klitzing, *Phys. Rev. Lett.* **96**, 126807 (2006).
¹⁵B. M. Ashkinadze, E. Linder, E. Cohen, and L. N. Pfeiffer, Proceedings of the 27th ICPS, Flagstaff (2004), Conference Pro-

- ceedings, 772, p. 511, (AIP Melville, New York, 2005) <http://proceedings.aip.org/proceedings>.
- ¹⁶J. H. Smet, B. Gorshunov, C. Jiang, L. Pfeiffer, K. West, V. Umankys, M. Dressel, R. Meisels, F. Kuchar, and K. von Klitzing, *Phys. Rev. Lett.* **95**, 116804 (2005).
- ¹⁷R. Meisels, I. Kulac, F. Kuchar, and M. Kriechbaum, *Phys. Rev. B* **61**, 5637 (2000).
- ¹⁸E. Olshanetsky, J. D. Caldwell, M. Pilla, Shu-chen Liu, C. R. Bowers, J. A. Simmons, and J. L. Reno, *Phys. Rev. B* **67**, 165325 (2003).
- ¹⁹D. A. Kleinman and R. C. Miller, *Phys. Rev. B* **32**, 2266 (1985).
- ²⁰M. Kozhevnikov, B. M. Ashkinadze, E. Cohen, and A. Ron, *Phys. Rev. B* **52**, 4855 (1995).
- ²¹B. M. Ashkinadze, E. Linder, E. Cohen, and L. N. Pfeiffer, *Phys. Rev. B* **71**, 045303 (2005).
- ²²G. A. Bastard, *Wave Mechanics Applied to Semiconductor Heterostructure* (Halsted Press, New York, 1991).
- ²³B. Couzinet, M. Dyakonov, A. Raymond, I. Elmezouar, M. Kamal-Saadib, and B. Etienne, *Solid State Commun.* **106**, 2638 (1998).
- ²⁴V. F. Gantmakher and Y. B. Levinson, *Carrier Scattering in Metals and Semiconductors* (North-Holland, Amsterdam, 1987).
- ²⁵V. Karpus, *Fiz. Tekh. Poluprovodn. (S.-Peterburg)* **22**, 151 (1988) [*Sov. Phys. Semicond.* **22**, 268 (1988)]; Cz. Jasiukiewicz and V. Karpus, *Semicond. Sci. Technol.* **11**, 1777 (1997).
- ²⁶*Phonon Scattering in Solids*, edited by L. J. Challis, V. W. Rampton, and A. F. G. Wyatt, (Plenum Press, New York, 1976).
- ²⁷E. L. Ivchenko and L. V. Takunov, *Fiz. Tverd. Tela (Leningrad)* **30**, 1161 (1988) [*Sov. Phys. Solid State* **30**, 671 (1988)].
- ²⁸G. Dresselhaus, A. F. Kip, and C. Kittel, *Phys. Rev.* **98**, 368 (1955).
- ²⁹S. J. Allen, H. L. Stormer, and J. C. M. Hwang, *Phys. Rev. B* **28**, 4875 (1983).
- ³⁰L. W. Engel, D. Shahar, C. Kurdak, and D. C. Tsui, *Phys. Rev. Lett.* **71**, 2638 (1993).
- ³¹C. Y. Hu, W. Ossau, D. R. Yakovlev, G. Landwehr, T. Wojtowicz, G. Karczewski, and J. Kossut, *Phys. Rev. B* **58**, R1766 (1998).
- ³²B. C. Cavenett, *Adv. Phys.* **30**, 475 (1981).
- ³³B. M. Ashkinadze, E. Linder, E. Cohen, V. V. Rudenkov, P. C. M. Christianen, J. C. Maan, and L. N. Pfeiffer, *Phys. Rev. B* **72**, 075332 (2005).